

# Optimization of Precursor Volume and its Impact on the Characterization of Copper Oxide Thin Films Deposited by Nebulizer Spray Pyrolysis Technique

V. Jagadeesan<sup>1</sup> and J. Charles Babu<sup>2\*</sup>

<sup>1</sup>Department of Electronics and Communication Engineering, P.S.G. College of Arts and Science, Coimbatore, Tamil Nadu, India

<sup>2</sup>Department of Electronics and Communication Systems, Sri Ramakrishna College of Arts and Science, Coimbatore, Tamil Nadu, India

## \*Correspondence to:

J. Charles babu  
Department of Electronics and  
Communication Systems,  
Sri Ramakrishna College of Arts and Science,  
Coimbatore, Tamil Nadu, India.  
E-mail: [charlesbabu@srcas.ac.in](mailto:charlesbabu@srcas.ac.in)

Received: January 03, 2024

Accepted: March 15, 2024

Published: March 20, 2024

**Citation:** Jagadeesan V, Babu JC. 2024. Optimization of Precursor Volume and its Impact on the Characterization of Copper Oxide Thin Films Deposited by Nebulizer Spray Pyrolysis Technique. *NanoWorld J* 10(S1): S241-S245.

**Copyright:** © 2024 Jagadeesan and Babu. This is an Open Access article distributed under the terms of the Creative Commons Attribution 4.0 International License (CCBY) (<http://creativecommons.org/licenses/by/4.0/>) which permits commercial use, including reproduction, adaptation, and distribution of the article provided the original author and source are credited.

Published by United Scientific Group

## Abstract

Nanoparticles of copper oxide (CuO) were synthesized and deposited on glass substrates using a standard nebulizer spray pyrolysis (NSP) process. The present study examined the impact of varying precursor volumes on the characteristics of CuO thin films formed by the NSP process. CuO thin films were developed in this work utilizing three distinct precursor volumes (3, 4, and 5 ml) using the NSP method. X-ray diffraction (XRD) analysis revealed a monoclinic crystal structure, which is consistent and proved by using JCPDS card no. (89-5899). The XRD studies have been used to calculate the dislocation density, micro-strain, and crystallite size. A surface profilometer was used to determine the average thickness. High-resolution Schottky emitter field emission-scanning electron microscope (FE-SEM) has been used to study morphological properties, and the results demonstrate that each film has been evenly deposited on the glass substrate. Energy dispersive X-ray (EDX) analysis has established the element's existence in the CuO thin films. Transmission values ranging from 20% to 65% at varied volumes were achieved, according to the optical measurements. Using Tauc plots, the energy band gaps were found to range from 1.85 eV to 2.15 eV, with the lowest band gap value of 1.85 eV for 4 ml. CuO thin-film's electrical conductivity was measured in DC, and the highest conductivity value for 4 ml was  $2.5 \times 10^{-8}$  S/cm.

## Keywords

Nanoparticles, Thin films, Copper oxide, X-ray diffraction, Field emission-scanning electron microscope, Electrical characteristics

## Introduction

Nanotechnology is a broad field of study that uses tiny particles in chemistry, biology, medicine, and material science, among other scientific disciplines. The development of metal and metal oxide nanoparticles with varying dimensions, morphologies, contrasts, and chemical compositions is the focus of nanotechnology. Major components of nanotechnology are nanoparticles, which are defined as atom clusters in the size range of 1 - 100 nm. The desirable characteristics of oxide metal-based thin films are mainly accountable for their use in many applications. CuO has been studied as a potentially useful nanomaterial for several purposes [1]. CuO nanoparticles are an energy-efficient and narrow band gap type p semiconductor with an elevated melting and boiling point, making it one of the strongest materials [2]. It is a semiconducting substance that is widely available, non-toxic, and easily synthesized at an inexpensive rate [3]. CuO nanoparticles have a narrow band gap value of 1.3 - 2.1 eV and a monoclinic structure [4]. CuO is useful in many different technological fields, including

renewable solar energy, sensors for gas detection, biological sensors, superconductors, light detectors, and energy-efficient substances [5-9]. There are numerous ways to synthesize CuO nanoparticles, and these include the following: spray pyrolysis, sol-gel, hydrothermal process, biological method, thermal plasma, solvothermal method, reactive magnetron sputtering, well diffusion method, microemulsions, and wet chemistry route [10-15]. NSP offers various benefits, including superior homogeneity control, seamless execution, and high purity. To carry out this study, CuO thin film deposits are made using a simple, economical, and efficient NSP process. Recent years have seen several investigations on the effects of deposition factors, including substrate temperature, molarity, doping, and precursor solution, on the characteristics of CuO films. Nevertheless, there aren't many reports on how the precursor solution's volume affects the characteristics of CuO thin films. The primary goal of this work is to act on various volumes of the precursor solution to synthesize nanostructure CuO thin films.

## Experimentation

### Preparation of precursor solution

For the synthesis of CuO nanoparticles, copper(II) nitrate ( $\text{Cu}(\text{NO}_3)_2 \cdot 3\text{H}_2\text{O}$ ) were used as a precursor material to obtain CuO nanoparticles. 0.3 M copper nitrate was well mixed in 20 ml of double distilled water with the assistance of magnetic stirrer. A magnetic stirrer was used to agitate the precursor solution for one hour. The final step was to prepare the blue color solution. At a substrate temperature of 450 °C, the CuO nanoparticles were deposited on the glass substrates using a standard NSP process.

### Deposition

Employing the NSP approach, CuO thin films have been produced on the surface of the glass substrate using different precursor volumes, namely 3 ml, 4 ml, and 5 ml. A nebulizer unit is coupled to an "L" shaped glass tube in an NSP system. Using a glass nozzle with an "L" shape, the solution that had been prepared was sprayed onto the glass substrate. Initially, the glass substrate was placed on the heated plate of the heater and 3 ml of the precursor solution was put in the bottom section of the nebulizer unit. With the use of a PID temperature controller, the heater's temperature was set at 450 °C. The distance of 5 cm between the glass tube nozzle and substrate was established. A compressed carrier gas air flow rate of 2.1 kg/cm<sup>2</sup> was found to be optimal. The solution was pumped towards the top of the nebulizer when the compressed air was discharged to the bottom side of the device. The solution began to migrate horizontally in the direction of the outlet as mist-like droplets the size of aerosols. Lastly, mist output from the nebulizer is directed through the spray nozzle and continually sprayed in a zigzag pattern on the glass substrate until the solution is sprayed completely. The 4 ml and 5 ml of CuO thin film were synthesized using a similar process.

### Characterization

Numerous analytical approaches have been employed to

evaluate the synthesized nonmaterial. XRD (Shimadzu, Japan) was employed to examine the crystalline size of the CuO nanoparticles and phase growth of the CuO thin films. The CuO thin-film morphology of the surface was examined using a high-resolution Schottky emitter FE-SEM. A visual representation of the elements' presence was provided by EDX. CuO thin-film optical characterization was studied using an ultraviolet-visible (UV-Vis) spectrometer (Jasco, Japan). Using a Keithley electrometer (6517-B), the CuO thin film's DC electrical characteristics were investigated.

## Results and Discussion

### Investigation on XRD

Figure 1 illustrates the impact of precursor volume on the structural characteristics of sprayed CuO thin films through varying the volume from 3 to 5 ml. The obtained CuO thin films are of the monoclinic crystal phase, according to the XRD images of the films that were obtained at different volumes. For all the films, the most significant peaks of 2θ value 32.60, 35.50, 38.70, and 52.70, which correspond to the (110), (-111), (111), and (020) planes, were seen. The values found in JCPDS card no. 89-5899 for the monoclinic form crystal phase in CuO thin films agreed with the diffraction peaks that were examined [4]. Table 1 displays the structural characteristics of CuO thin films. Table 1 displays the average thickness of the 3 ml, 4 ml, and 5 ml sprayed CuO thin films as determined by the surface profilometer.

For the structural investigation, the average crystallite size was calculated using Scherrer's formula [16] to determine the full-width half maximum (FWHM) value.

$$D = \frac{0.9\lambda}{\beta \cos \theta} \quad (1)$$

Where 'D' is the estimated crystallite size, 'θ' is the Bragg angle, 'λ' is the X-ray wavelength, and 'β' is the FWHM.

The average crystallite size of the various films, which

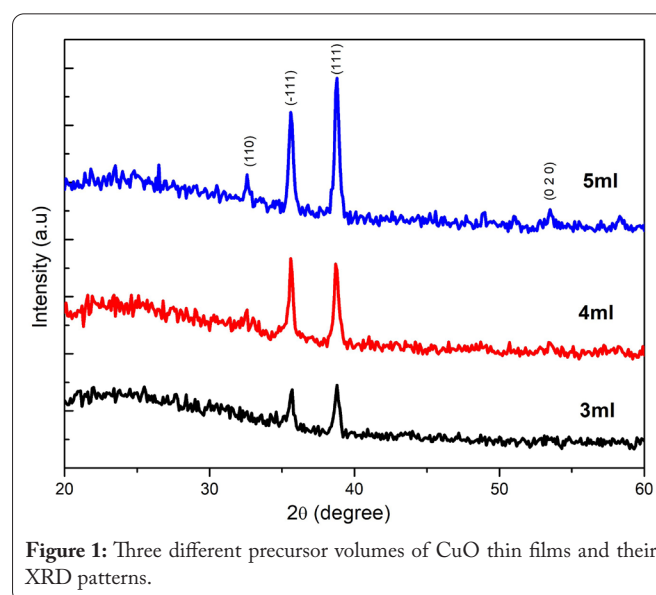


Figure 1: Three different precursor volumes of CuO thin films and their XRD patterns.

**Table 1:** Physical parameters of NSP prepared CuO thin films.

Volume	2θ (°)	FWHM (°)	Crystallite size (D) (nm)	Film thickness (nm)	Micro-strain (ε)	Dislocation density (δ) (x 10 <sup>15</sup> lines m <sup>-2</sup> )
3 ml	38.7547	0.4366	19	105	0.0017	2.68404
4 ml	38.7277	0.4518	18	109	0.0018	2.87466
5 ml	38.7527	0.3661	23	120	0.0015	1.88724

were made by the NSP process with varying volumes, ranges from 18 to 23 nm and is shown in table 1. The 4 ml sample is found to have a smaller crystallite size. It was evident that the precursor volume controlled the crystallite size and had a crucial role. Figure 2 shows how the FWHM, and average crystallite size varies. The formula below was also used to assess the micro-strain (ε) and dislocation density (δ) [17-19].

$$\epsilon = \frac{\beta \cos \theta}{4} \quad (2)$$

$$\alpha = \frac{1}{D^2} \quad (3)$$

Figure 3 depicts the variations of micro-strain as well as the average crystallite size. According to the results, the 4 ml of precursor volume in this investigation provided good crystalline character. The significant improvement observed in the prepared thin films was attributed to the nanoparticle size and monoclinic crystal phase structure of the CuO thin films.

### FE-SEM and EDX investigations

The developed CuO thin film's surface morphology and chemical constituents were examined using EDX and high-resolution Schottky emitter FE-SEM. The FE-SEM data obtained in figure 4 show how the morphological parameters of the CuO thin film vary with precursor volume. NSP coating methods coat the substrate surface with a uniform, smooth coating. The benefit of using the NSP process is its uniform coating. It is evident from FE-SEM images that there are no breaks in any of the films. CuO thin films are observed to be well-covered and uniformly attached to the substrate, exhibiting the morphological characteristics of an FE-SEM. The EDX spectra of developed CuO thin films, which reveal the presence of oxygen and copper (Cu), are displayed in figure 5. Using EDX analysis, the atomic agglutinate of Cu and O were found in the inset of figure 5. It is verified that the produced nanoparticles are in fact copper oxide by the predominance of Cu and O in every plot.

### UV-Vis spectrophotometer investigation

Using a UV-Vis spectrophotometer, both optical transmittance and absorption were investigated. Figure 6a exhibits the optical transmittance formed in the wavelength range of 300 - 1200 nm using varying precursor volumes of 3 ml, 4 ml, and 5 ml. A UV absorption peak of 289 nm was recorded for CuO nanoparticles synthesized by NSP process. The films' visibility ranged from 20% to 65%. At the lowest volume (3 ml), the CuO thin film's highest transparency was recorded. Figure

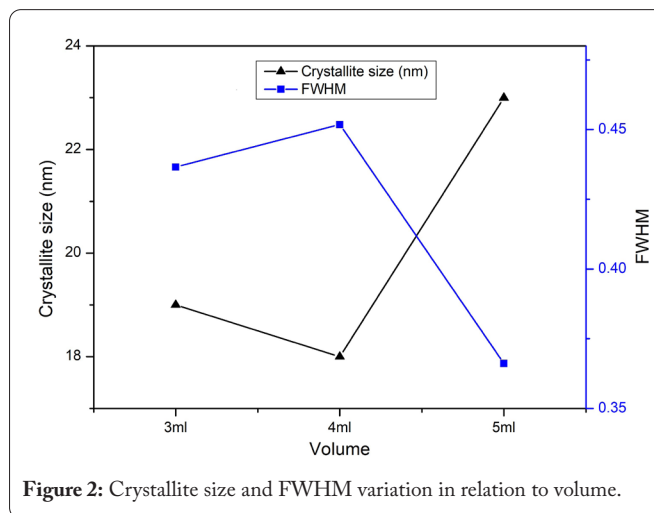


**Figure 2:** Crystallite size and FWHM variation in relation to volume.

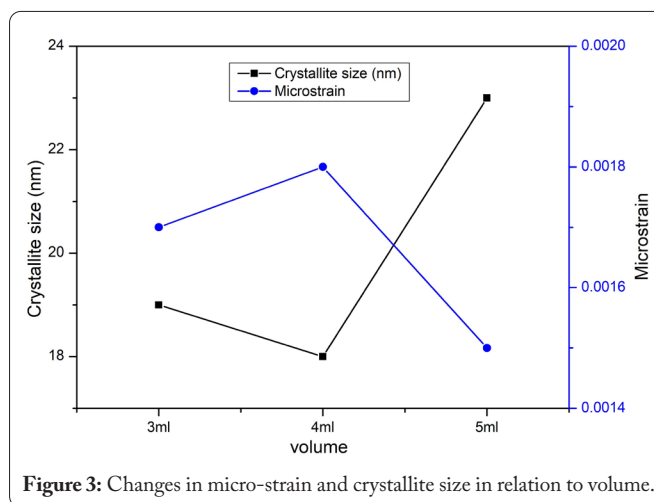


**Figure 3:** Changes in micro-strain and crystallite size in relation to volume.

6b illustrates the absorption of the prepared films formed with varying volumes. The absorption of the NSP-prepared films was found to be low in the visible spectrum and high in the UV spectrum. The absorption plot made it abundantly evident that as volume increased, so did the CuO thin film absorbance. At the largest precursor volume of 5 ml, the maximum absorbance value was recorded. Because of this, it is widely known that the volume of the solution has a significant impact on the optical characteristics of the CuO nanoparticles in the films, as does the transparency and absorption.

Tauc's relation was used to calculate the optical band gap value based on absorption versus wavelength spectra. Since CuO has a narrow band gap, the band gap energy (Eg) and absorption coefficient can be determined using the following formula, which is based on Tauc's relationship [20].

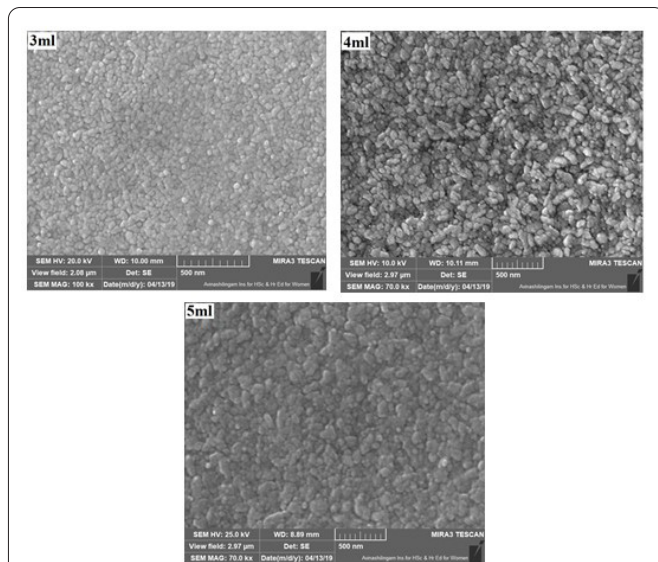


Figure 4: FE-SEM pictures of NSP prepared CuO thin film samples deposited with varying precursor volumes.

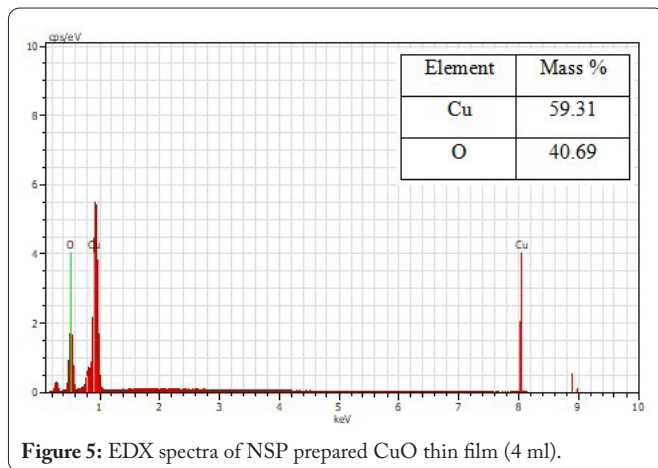


Figure 5: EDX spectra of NSP prepared CuO thin film (4 ml).

$$\alpha hv = B(hv - E_g)^n \quad (4)$$

Where ‘ $\alpha$ ’ is the absorption coefficient, and the formula below can be used to determine it.

$$A = 2.303A/t \quad (5)$$

Where ‘ $t$ ’ is the CuO film thickness and ‘ $A$ ’ is the absorbance value.

In figure 7, the relationship between  $(\alpha hv)^2$  and  $hv$  was displayed. The computed values of the energy band gap for NSP prepared CuO thin films were 2.15 eV, 1.85 eV, and 1.93 eV for 3 ml, 4 ml, and 5 ml, respectively, based on the Tauc’s plot.

### DC electrical conductivity investigation

DC electrical conductivity was measured at room temperature using a two-probe Keithley electrometer 6517-B set-up. As seen in figure 8a, the current values were measured for various applied voltages ranging from 1 to 10 V. According

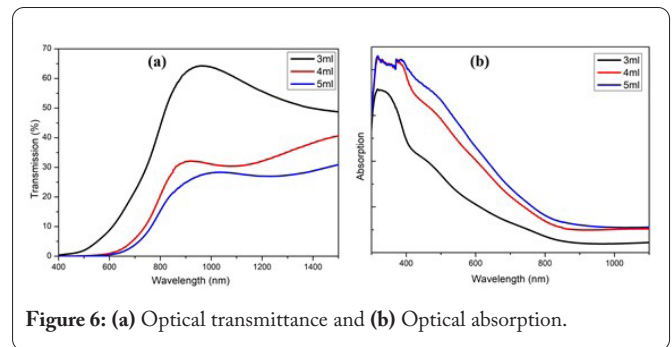


Figure 6: (a) Optical transmittance and (b) Optical absorption.

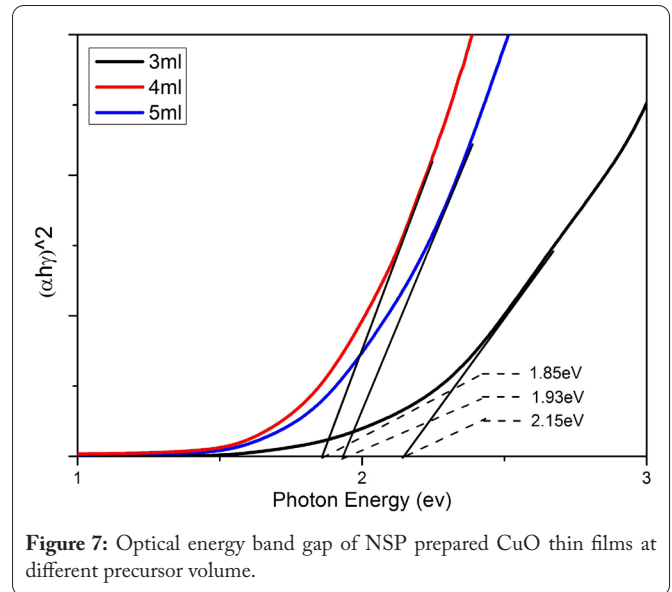


Figure 7: Optical energy band gap of NSP prepared CuO thin films at different precursor volume.

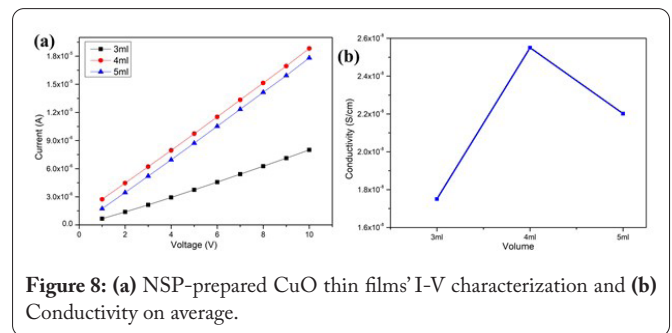


Figure 8: (a) NSP-prepared CuO thin films' I-V characterization and (b) Conductivity on average.

to figure 8a, the current values increased progressively as the applied voltage increased. The following formula was used to determine the DC conductivity of NSP-prepared CuO thin films at different volumes [4].

$$\sigma = \left(\frac{V}{I}\right) \times \left(\frac{d}{A}\right) \quad (6)$$

Where ‘ $A$ ’ is the film’s cross-sectional area, ‘ $d$ ’ is the inter-probe distance, ‘ $I$ ’ is the current, and ‘ $V$ ’ is the applied voltage.

Figure 8b displays the I-V properties of NSP-prepared CuO thin films at different volumes. For 4 ml, the highest conductivity value was  $2.5 \times 10^{-8}$  S/cm. The outcome showed that the CuO thin film’s conductivity climbed for 4 ml and declined for 5 ml.

## Conclusion

Nanoparticles of CuO were synthesized and deposited on glass substrates using a standard NSP process. The present investigation employed an easy-to-use, economical NSP approach for developing CuO thin films with varying precursor volumes. Precursor volume's impact on CuO thin film characteristics has been studied. All the films were found to be monoclinic crystal phases by structural analysis. The crystalline size of CuO nanoparticles was estimated using XRD analysis. The sizes of the crystallites range from 19, 18, and 23 nm for 3 ml, 4 ml, and 5 ml, respectively. The significant improvement observed in the prepared thin films was attributed to the nanoparticle size and monoclinic crystal phase structure of the CuO thin films. The substrate surface has a homogenous and smooth covering, as seen in the FE-SEM images. According to the optical analysis, CuO thin film optical transmittance reduced as volume increased. The CuO thin film's highest transparency was recorded at the lowest volume of 3 ml. The absorption study unequivocally showed that the absorbance of the NSP-prepared CuO thin films increased along with the volume. Each CuO thin film has a substantial absorption in the visible range and a narrow band gap. For 3 ml, 4 ml, and 5 ml, the measured band gap values for CuO thin films were 2.15 eV, 1.85 eV, and 1.93 eV, respectively. The prepared films' DC electrical conductivity shows that the CuO thin film's conductivity increases for 4 ml and decreases for 5 ml. It is discovered that a 4 ml precursor volume for CuO thin film is ideal, and at this point, the best-performing film has been produced.

## Acknowledgments

None.

## Conflict of Interest

None.

## References

- Purusottam Reddy B, Sivajee Ganesh K, Hussain OM. 2016. Growth, microstructure and super capacitive performance of copper oxide thin films prepared by RF magnetron sputtering. *Appl Phys A* 122: 128. <https://doi.org/10.1007/s00339-015-9588-z>
- Alkoy EM, Kelly PJ. 2005. The structure and properties of copper oxide and copper aluminium oxide coatings prepared by pulsed magnetron sputtering of powder targets. *Vacuum* 79(3-4): 221-30. <https://doi.org/10.1016/j.vacuum.2005.03.011>
- Zeggar ML, Bourfaa F, Adjimi A, Aida MS, Attaf N. 2016. Copper oxide thin films for ethanol sensing. *IOP Conf Ser Mater Sci Eng* 108(1): 012004. <https://doi.org/10.1088/1757-899X/108/1/012004>
- Jagadeesan V, Subramaniam V. 2019. Impact of molarity on structural, optical, morphological and electrical properties of copper oxide thin films prepared by cost effective jet nebulizer spray pyrolysis technique. *J Mater Sci* 30: 1571-1578. <https://doi.org/10.1007/s10854-018-0428-8>
- Richardson TJ, Slack JL, Rubin MD. 2001. Electrochromism in copper oxide thin films. *Electrochem Acta* 46(13-14): 2281-2284. [https://doi.org/10.1016/S0013-4686\(01\)00397-8](https://doi.org/10.1016/S0013-4686(01)00397-8)
- Fujimoto K, Oku T, Akiyama T, Suzuki A. 2013. Fabrication and characterization of copper oxide-zinc oxide solar cells prepared by electrodeposition. *J Phys* 433(1): 012024. <https://doi.org/10.1088/1742-6596/433/1/012024>
- Omayio EO, Karimi PM, Njoroge WK, Mugwanga FK. 2013. Current-voltage characteristics of p-CuO/n-ZnO: Sn Solar cell. *Int J Thin Film Sci Technol* 2(1): 25-28.
- Zhang X, Song J, Jiao J, Mei X. 2010. Preparation and photocatalytic activity of cuprous oxides. *Solid State Sci* 12(7): 1215-1219. <https://doi.org/10.1016/j.solidstatesciences.2010.03.009>
- Johan MR, Suan MS, Hawari NL, Ching HA. 2011. Annealing effects on the properties of copper oxide thin films prepared by chemical deposition. *Int J Electrochem Sci* 6(12): 6094-6104. [https://doi.org/10.1016/S1452-3981\(23\)19665-9](https://doi.org/10.1016/S1452-3981(23)19665-9)
- Rastkar AR, Niknam AR, Shokri B. 2009. Characterization of copper oxide nanolayers deposited by direct current magnetron sputtering. *Thin Solid Films* 517(18): 5464-5467. <https://doi.org/10.1016/j.tsf.2009.01.095>
- Balamurugan B, Mehta BR. 2001. Optical and structural properties of nanocrystalline copper oxide thin films prepared by activated reactive evaporation. *Thin Solid Films* 396(1-2): 90-96. [https://doi.org/10.1016/S0040-6090\(01\)01216-0](https://doi.org/10.1016/S0040-6090(01)01216-0)
- Bayansal F, Şahin B, Yüksel M, Çetinkara HA. 2014. Modification of morphological, structural, and optical properties of SILAR-based growth of CuO films on glass-slides by addition of dextrin. *J Alloys Compd* 614: 379-382. <https://doi.org/10.1016/j.jallcom.2014.06.123>
- Akgul FA, Akgul G, Yildirim N, Unalan HE, Turan R. 2014. Influence of thermal annealing on microstructural, morphological, optical properties and surface electronic structure of copper oxide thin films. *Mater Chem Phys* 147(3): 987-995. <https://doi.org/10.1016/j.matchemphys.2014.06.047>
- Zappa D, Comini E, Zamani R, Arbiol J, Morante JR, et al. 2011. Copper oxide nanowires prepared by thermal oxidation for chemical sensing. *Procedia Eng* 25: 753-756. <https://doi.org/10.1016/j.proeng.2011.12.185>
- Morales J, Sanchez L, Martin F, Ramos-Barrado JR, Sanchez M. 2005. Use of low-temperature nanostructured CuO thin films deposited by spray-pyrolysis in lithium cells. *Thin Solid Films* 474(1-2): 133-140. <https://doi.org/10.1016/j.tsf.2004.08.071>
- Siddiqui H, Qureshi MS, Haque FZ. 2016. Surfactant assisted wet chemical synthesis of copper oxide (CuO) nanostructures and their spectroscopic analysis. *Optik* 127(5): 2740-2747. <https://doi.org/10.1016/j.ijleo.2015.11.220>
- Mariappan R, Ragavendar M, Ponnuswamy V. 2011. Growth and characterization of chemical bath deposited Cd<sub>1-x</sub>Zn<sub>x</sub>S thin films. *J Alloys Compd* 509(27): 7337-7343. <https://doi.org/10.1016/j.jallcom.2011.04.088>
- Kasar RR, Deshpande NG, Gudage YG, Vyas JC, Sharma R. 2008. Studies and correlation among the structural, optical and electrical parameters of spray-deposited tin oxide (SnO<sub>2</sub>) thin films with different substrate temperatures. *Phys B Condens Matter* 403(19-20): 3724-3729. <https://doi.org/10.1016/j.physb.2008.06.023>
- Shkir M, AlFaify S. 2017. Tailoring the structural, morphological, optical and dielectric properties of lead iodide through Nd<sup>3+</sup> doping. *Sci Rep* 7(1): 16091. <https://doi.org/10.1038/s41598-017-16086-x>
- Chand P, Gaur A, Kumar A, Gaur UK. 2015. Effect of NaOH molar concentration on morphology, optical and ferroelectric properties of hydrothermally grown CuO nanoplates. *Mater Sci Semicond Process* 38: 72-80. <https://doi.org/10.1016/j.mssp.2015.04.006>